JACS Au
AN OPEN ACCESS JOURNAL OF THE AMERICAN CHEMICAL SOCIETY

pubs.acs.org/jacsau
Article

Selective Arene Photonitration via Iron-Complex β-Homolysis

Shuyang Liu, Ziyu Gan, Min Jiang, Qian Liao, Yusheng Lu, Hongyao Wang, Zhiyan Xue, Ziyang Chen, Yongqiang Zhang, Xiaobo Yang, Chunying Duan, and Yunhe Jin*

Cite This: JACS Au 2024, 4, 4899−4909
Read Online

ACCESS | Metrics & More | Article Recommendations | Supporting Information

ABSTRACT: Nitroaromatics, as an important member and source of nitrogen-containing aromatics, is bringing enormous economic benefits in fields of pharmaceuticals, dyes, pesticides, functional materials, fertilizers, and explosives. Nonetheless, the notoriously polluting nitration industry, which suffers from excessive discharge of fumes and waste acids, poor functional group tolerance, and tremendous purification difficulty, renders mild, efficient, and environmentally friendly nitration a formidable challenge. Herein, we develop a visible-light-driven biocompatible arene C−H nitration strategy with good efficiency and regioselectivity, marvelous substrate applicability and functional group tolerance, and wide application in scale-up synthesis, total synthesis, and late-stage functionalization. A nitryl radical delivered through unusual β-homolysis of a photoexcited ferric-nitrate complex is proposed to be the key nitrification reagent in this system.

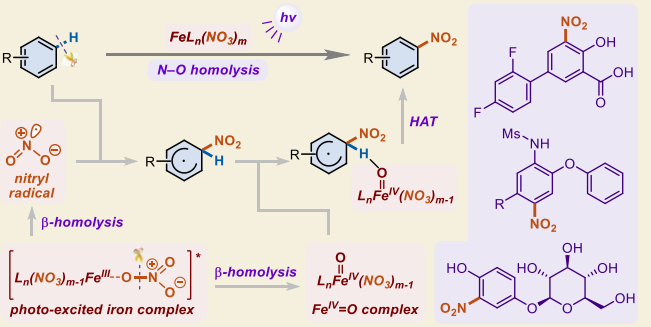

KEYWORDS: *photochemistry, β-homolysis, nitryl radical, arene nitration, late-stage functionalization*

INTRODUCTION

Nitrogen-containing aromatic compounds, a family composed of dozens of extensively existing core structures, are among the largest volume commodity chemicals used in the manufacture of pharmaceuticals, dyes, pesticides, functional materials, fertilizers, and explosives (Figure 1a).[1] For instance, over 130 of the top 200 small molecule drugs by retail sales in 2022 belong to this family, occupying 77.6% of the total sales with the figure up to 253.5 billion (US dollars).[2] Arene nitration has been a widely used nitrogen-introducing method and an immensely important industrial process for decades, with the global sales of only nitrobenzene estimated to approach $10 billion in 2023.[3] Diverse well-established transformations from nitro groups to other nitrogen-containing functional groups render nitroaromatics a key building block and intermediate in organic synthesis.[1] Furthermore, the landscape of molecular synthesis has gained major impetus by the introduction of late-stage functionalization (LSF) methodologies over the past decade.[4] Among diversified LSF strategies, direct modification of inert C−H bonds in a selective manner, which sets the stage for unconceived retrosynthetic disconnections, takes advantage of the availability of complex molecules as starting materials and makes previously unsynthesizable scaffolds accessible. Therefore, C(sp^2)−H nitration as a significant LSF method with enormous economic benefits has attracted scientists' great efforts. As shown in Figure 1b, the nitroaromatic production traditionally relied on aromatic electrophilic substitution of nitronium ions (NO_2^+) delivered by the "mixed acid" approach with concentrated sulfuric and nitric acids.[5] Just because of this, the nitration industry, a valuable but notoriously polluting process, suffers from the excessive discharge of nitrogen oxide (NO_x) fumes and waste acids, poor functional group tolerance resulting from superstoichiometric amounts of acid and harsh conditions, and tremendous difficulty on isomer purification up to now.[6] To cross these hurdles, many improvements were proposed unremittingly in the past few decades.[7] Various presynthesized organic nitrating agents and activating methods for metal nitrates including ferric ones were impressively developed for the efficient generation of nitronium ions under thermal conditions by Katayev and co-workers in recent years.[8] Metal-catalyzed C(sp^2)−H activation at the *ortho*-position of a directing group is another effective strategy for selective nitration.[9] Except for the polar pathway, some electron-rich aromatics can also be directly nitrated through a radical intermediate. The existing methods for nitryl radical generation mainly depended on the oxidative decomposition of *tert*-butyl nitrite, the thermal decomposition of ferric nitrate, and single electron oxidation of nitrites (Figure 1c).[8g,9,10] Nevertheless, several problems still exist, such as indispensable substrate prefunctionalization, harsh reaction conditions (high

Received: September 21, 2024
Revised: November 9, 2024
Accepted: November 11, 2024
Published: November 21, 2024

https://doi.org/10.1021/jacsau.4c00880
JACS Au 2024, 4, 4899−4909

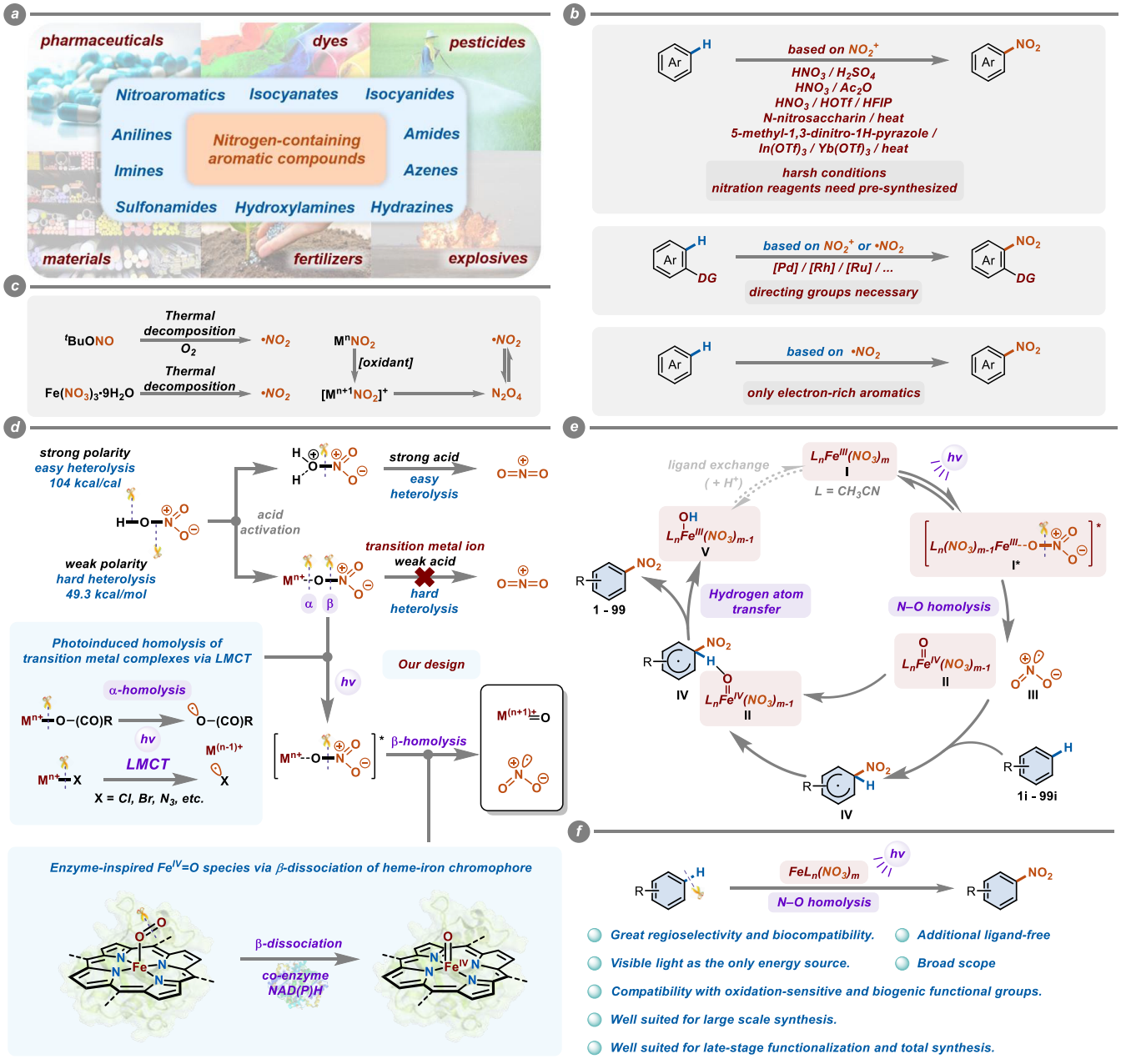

Figure 1. Introduction and our design. (a) Applications for nitroarenes. (b) Previous protocols for arene nitration. (c) Approaches for generating nitryl radicals. (d) Challenges and our design for nitrate activation under mild conditions. (e) General design plan for the mechanisms of arene photonitration via iron-complex *β*-homolysis. (f) This work.

temperature and strong acid), usage and unrecyclability of noble metal catalysts (Pd, Rh, and Ru), and limited reaction scopes, posing a formidable challenge of developing mild, efficient, and environmentally friendly nitration protocols to meet the requirements of green and circular economy.

To address this long-standing issue, we focused our attention back on the basic molecular structure of nitric acid, the most low-cost commercial nitrification reagent, to look for clues. As displayed in Figure 1d, the polarity of the O−H bond in HNO_3 is obviously stronger than that of the neighboring N−O bond, endowing the O−H bond with an easy-heterolysis characteristic responsible for the acidity of nitric acid. However, the generation of an active nitration species NO_2^+ requires a challenging heterolysis process of the N−O bond with weak polarity. The ingenious solution from the "mixed acid" approach is to form an oxonium ion with the help of strong Brønsted acid H_2SO_4 to enhance the N−O bond polarity,[5] but bringing serious pollution problems at the same time. To avoid the employment of excess acids, we planned to choose transition metal ions instead of protons as nitrate-activating reagents to cut off the weakly polar bond. Regrettably, the Lewis acidities, which are equivalent to the degrees of electron deficiency, of transition metal ions are always insufficient to realize N−O heterolysis directly under mild conditions. Recently, the rapid development of photocatalysis science,[11] especially on photoactive complexes with earth-abundant metals[12] affords us new opportunities to get out of this dilemma. Numbers of simple complexes of cheap

https://doi.org/10.1021/jacsau.4c00880
JACS Au 2024, 4, 4899−4909

Table 1. Optimization of Reaction Conditions[a,b]

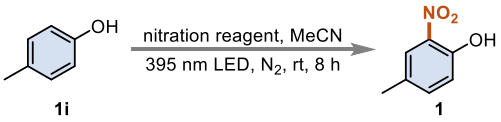

1i 1

entry	nitration reagent	yields [%]
1	$Fe(NO_3)_3{\cdot}9H_2O$ (0.4 equiv)	92
2	$Fe(NO_3)_3{\cdot}9H_2O$ (0.5 equiv)	85
3	$Cu(NO_3)_2{\cdot}3H_2O$ (0.7 equiv)	23
4	$Co(NO_3)_2{\cdot}6H_2O$ (0.7 equiv)	trace
5	$NaNO_3$ (1.5 equiv)	N.R.
6	$Fe(NO_3)_3{\cdot}9H_2O$ (0.1 equiv) + $NaNO_3$ (1.2 equiv)	16
7	$Fe_2(SO_4)_3$ (0.2 equiv) + $NaNO_3$ (2 equiv)	trace
8	$Fe_2(SO_4)_3$ (0.2 equiv) + NBu_4NO_3 (2 equiv)	N.R.
9	$Fe(NO_3)_3{\cdot}9H_2O$ (0.1 equiv) + HNO_3 (1 equiv)	25
10	$Fe(NO_3)_3{\cdot}9H_2O$ (0.1 equiv) + $NaNO_3$ (1 equiv) + MsOH (1 equiv)	47

[a]Standard conditions: **1i** (0.2 mmol), nitration reagent, MeCN (2 mL), 395 nm LED, N_2, room temperature, 8 h. [b]^{1}H NMR yield. N.R.: No reaction.

transition metals were reported to be able to perform a distinctive photoinduced homolysis process called ligand−metal charge transfer (LMCT) by Doyle,[13] Molander,[14] Nocera,[15] Zuo,[16] and many other distinguished groups[17] including us.[17d−f] LMCT excitations tend to promote α homolysis of the metal−ligand bond, leading to the generation of a reduced metal complex together with a ligand-centered radical. This unique and straightforward photoexcitation has attracted significant research attention from synthetic chemists in recent years. Various heteroatom-center radicals given by this tactic under light irradiation have been widely applied in many fields of synthetic chemistry such as hydrocarbon activation,[13−16,17a] and olefin functionalization.[17k−s] Nonetheless, an analogous α-homolysis of our desired metal-nitrate complex will not provide any serviceable nitration agent. An enlightening inspiration for this issue is from an elementary catalytic procedure of natural cytochrome P450 enzyme that a specific β-dissociation will occur after the combination of multinitrogen-coordinated heme-iron center and oxygen with the assistance of coenzyme NADPH.[18] With a similar pattern, we reasonably anticipated a rarely reported β-homolysis of a N−O single bond in a photoactivated iron-nitrate complex with acetonitrile as the solvent and a dynamic ligand, generating a Fe^{IV}=O species and a nitration agent $\cdot NO_2$. Another clue from the nitric acid's molecular structure is the weak bond dissociation energy (BDE) of the N−O single bond (49.3 kcal/mol),[19] which naturally suggests a potential easy-homolysis property instead of heterolysis.

According to the above thoughts, a proposed mechanism for arene photonitration *via* iron-complex β-homolysis is envisioned in Figure 1e. Initially, a photoactive complex **I** composed of a ferric ion center and several nitrate/acetonitrile ligands was reversibly stimulated to reach an excited state **I*** under light irradiation.[12] A spontaneous N−O homolysis released a desired nitryl radical **III** and a Fe^{IV}=O complex **II** that has been demonstrated as a crucial intermediate for direct C(sp^3)−H[18b,c,20] and C(sp^2)−H[21] cleavage. A subsequent electrophilic addition between an electron-deficient radical **III** and an electron-rich arene substrate resulted in a cyclic radical **IV**.[22] Compared to the "mixed acid" approach, the essential hydrogen atom dissociation step from **IV** to the nitroaromatic product reflects a higher degree of difficulty than the corresponding deprotonation step in the NO_2^+ pathway. Fortunately, the strong hydrogen-atom-transfer (HAT) ability of **II** can easily get over this barrier.[18b,c,20] Finally, the resulting iron complex **V** from HAT may undergo an in situ ligand exchange assisted by the additional acid for regenerating the photoactive complex **I**. On the basis of the aforementioned design, we herein achieved photoinduced radical-mediated nitration of arenes with good regioselectivity and biocompatibility, a broad scope, ample functional group tolerance, and wide application in synthesis (Figure 1f).

RESULTS AND DISCUSSION

Condition Optimization

According to our design, we initiated our study with a commercial Fe−NO_3 complex, ferric nitrate, as the nitro source, and MeCN as the solvent. Satisfyingly, the model reaction from *p*-cresol (**1i**) to 4-methyl-2-nitrophenol (**1**) with $Fe(NO_3)_3{\cdot}9H_2O$ (0.4 equiv, equivalent to NO_3^- 1.2 equiv) under irradiation of 395 nm LEDs afforded a satisfactory yield of 92% (Table 1, entry 1). Further increasing the equivalents of $Fe(NO_3)_3{\cdot}9H_2O$ did not provide an enhanced yield (entry 2). Kinds of metal nitrates including $Cu(NO_3)_2{\cdot}3H_2O$, $Co(NO_3)_2{\cdot}6H_2O$, and $NaNO_3$ were tested then, but only copper nitrate could give the corresponding product in a low yield (entries 3−5) probably because of the similar photoexcited property between iron and copper.[17a,d,y] Simple combinations of catalytic ferric salts [$Fe(NO_3)_3{\cdot}9H_2O$, $Fe_2(SO_4)_3$] and other nitrates ($NaNO_3$, NBu_4NO_3) appear to be unsuccessful due to the low interaction rate between each other thanks to the poor solubility of these salts in MeCN (entries 6−8). We also attempted to conduct the reaction with a catalytic amount of $Fe(NO_3)_3{\cdot}9H_2O$ and equivalent nitrate anions as the nitro source under slightly acidic conditions, and the yields of the corresponding product can only reach a moderate level (entries 9−10). Different types of solvents were also examined, showing acetonitrile to be the best choice (see details in the Supporting Information, Table S1, entries 11−15). Applying mixed solvents of MeCN and water or DMSO which are well-known good solvents for metal salts made no improvement in yields (Table S1, entries 16−17). Variations in illumination wavelengths and atmospheres exhibited no positive effects (Table S1, entries 18−21). Finally, a control experiment

https://doi.org/10.1021/jacsau.4c00880
JACS Au 2024, 4, 4899−4909

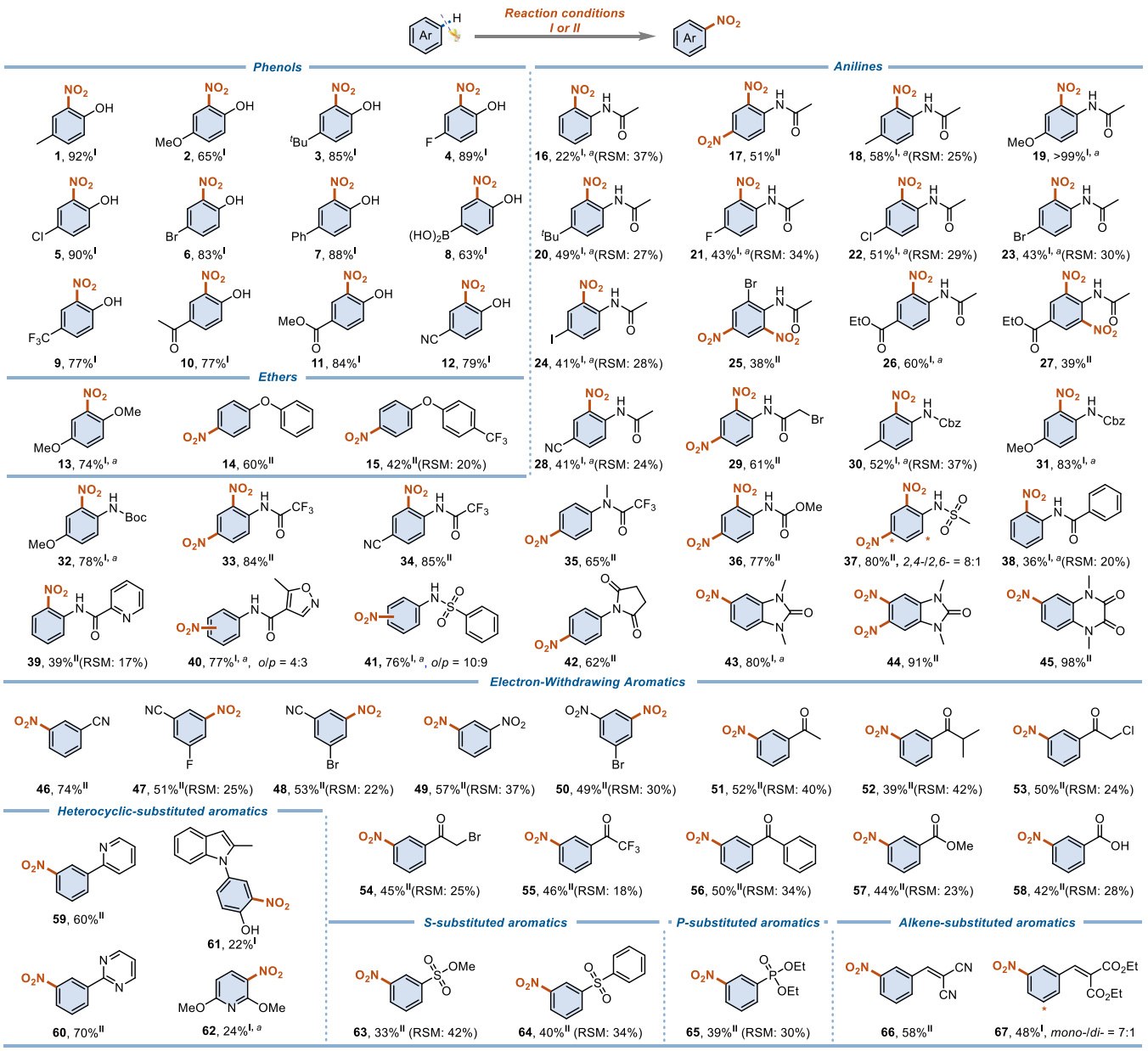

Figure 2. Substrate scope of simple arenes. Reaction conditions: I: Arene (0.2 mmol), $Fe(NO_3)_3{\cdot}9H_2O$ (0.4 equiv) ([a]$Fe(NO_3)_3{\cdot}9H_2O$ 0.5 equiv), MeCN (2 mL), N_2, rt, 395 nm LEDs, 8 h; II: Arene (0.2 mmol), $Fe(NO_3)_3{\cdot}9H_2O$ (1.5 equiv), MsOH (1.1 equiv), MeCN (2 mL), O_2, rt, 395 nm LEDs, 8 h. RSM, recovered starting material.

indicated that the reaction would not occur without visible light as an energy source (Table S1, entry 22).

Substrate Scope Scanning

With the optimized reaction conditions in hand, a broad range of arenes were selected as subjects to examine the generality of our protocol. As shown in Figure 2, a large number of simple arenes with electron-donating groups, including phenols, ethers, and anilines, were tried first, delivering the corresponding nitroaromatics in moderate to excellent yields (**1**−**45**). Most products could be obtained in a single isomer, and the regioselectivity of different positions appeared to be governed by the electronic properties of substituents in a similar fashion to electrophilic aromatic substitution.[1a] As vital synthons, halogen-substituted aromatics were all suitable substrates to furnish multifunctionalized products (**4**−**6**, **21**−**25**), offering a good chance for further derivatization. Meanwhile, their useful Suzuki-Miyaura-coupling partner,[1a] arylboronic acid, also supplied the nitrated product (**8**) in a good yield without any requirement of protecting groups. The introduction of strong electron-withdrawing substituents, such as trifluoromethyl, acetyl, ester, and cyano groups, just brought little negative influence on yields (**9**−**12**, **26**−**29**, **34**). Nitrated anilines protected by various groups including *α*-bromoacetyl (**29**), benzyloxy-carbonyl (**30**, **31**), *tert*-butoxycarbonyl (**32**), trifluoroacetyl (**33**−**35**), methoxy-carbonyl (**36**), sulfonyl (**37**, **41**), benzoyl (**38**), and heterocycloformyl (**39**, **40**) were synthesized efficiently as well, implying that our method has tremendous potential in LSF of natural products such as peptides. Derivatives of benzoimidazole and quinoxaline rings were employed next, and the corresponding products were achieved in excellent yields (**43**−**45**). Notably, mono- or dinitration could be conveniently modulated for selected

https://doi.org/10.1021/jacsau.4c00880
JACS Au 2024, 4, 4899−4909

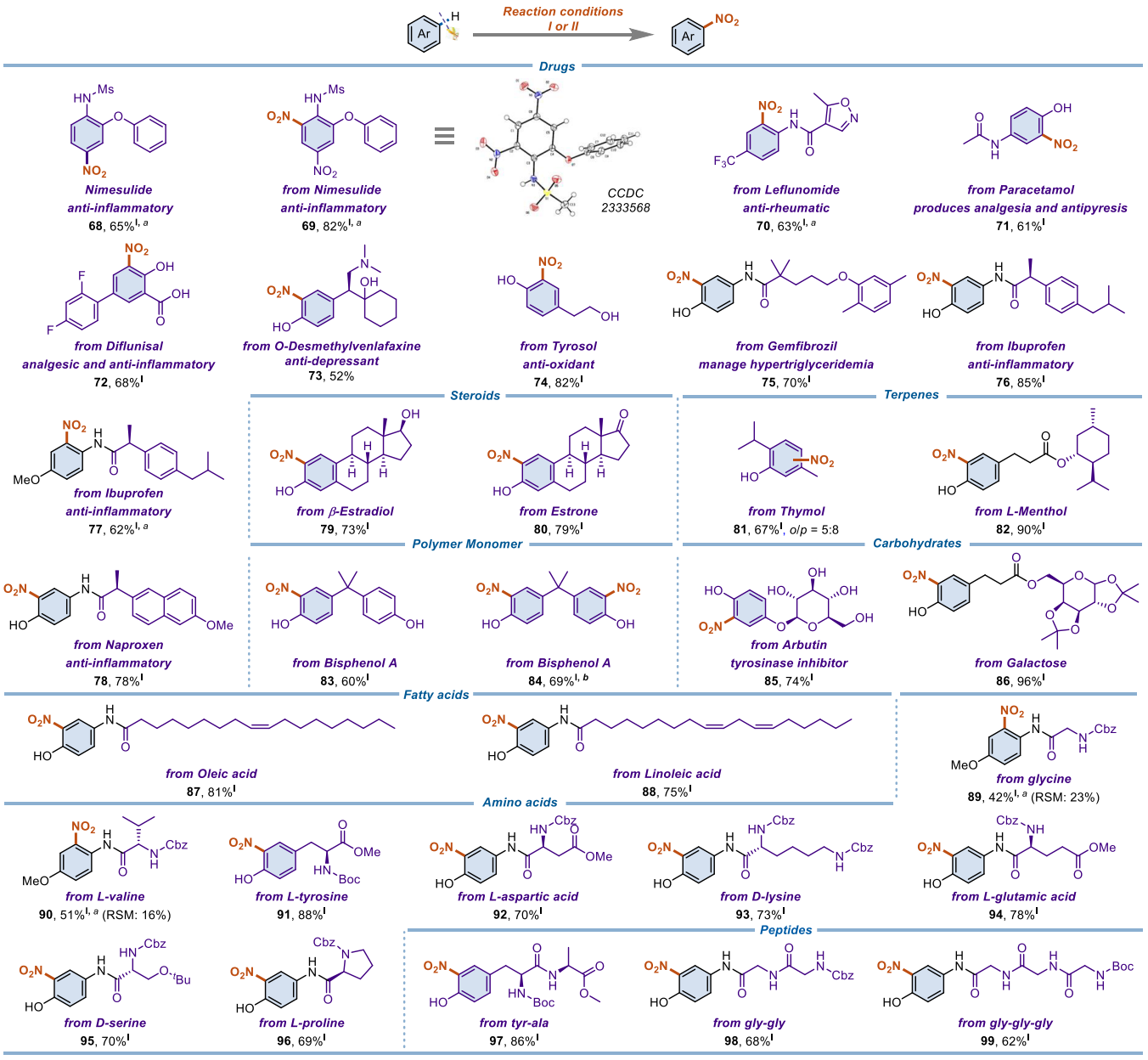

Figure 3. Late-stage photonitration of drugs, polymer monomer, and biorelevant compounds. Reaction conditions: I: Arene (0.2 mmol), $Fe(NO_3)_3{\cdot}9H_2O$ (0.4 equiv) ([a]$Fe(NO_3)_3{\cdot}9H_2O$ 0.5 equiv; [b]$Fe(NO_3)_3{\cdot}9H_2O$ 0.7 equiv), MeCN (2 mL), N_2, rt, 395 nm LEDs, 8 h; II: Arene (0.2 mmol), $Fe(NO_3)_3{\cdot}9H_2O$ (1.5 equiv), MsOH (1.1 equiv), MeCN (2 mL), O_2, rt, 395 nm LEDs, 8 h. RSM, recovered starting material.

examples by usage of different equivalences of ferric nitrate (**16** and **17**, **26** and **27**, and **43** and **44**). According to the fundamental characteristics of electrophilic aromatic substitution,[1a] direct nitration of strongly electron-deficient arenes presents more challenges as well as more research values than those of electron-rich ones, especially via a nitryl radical pathway. After proper adjustment of reaction conditions (Table S2), the nitration goals of diverse electron-deficient arenes were successfully reached in good to moderate yields with excellent regioselectivity and functional group tolerance (**46**–**67**). Plenty of substituents applicable for postmodification in synthetic methodology, including nitriles (**46**–**48**), nitroarenes (**49**, **50**), ketones (**51**–**56**), ester (**57**), benzoic acid (**58**), benzenesulfonate (**63**), and phenylphosphonate (**65**) were all compatible, providing the *meta*-nitrated products in good isolated yields.

Furthermore, the well-known active aryl/alkyl halides (F, Cl, and Br) (**47**, **48**, **50**, **53**, and **54**) and olefins (**66 and 67**) showed good stability under these conditions, providing a huge space for further cross-couplings. Two frequently used directing groups in transition-metal catalysis, pyridin-2-yl and pyrimidin-2-yl, were, respectively, assembled on benzenes as substrates, and the nitration transformation still proceeded well at *meta*-position (**59 and 60**). As valuable heteroaromatics, indole and pyridine were next involved, and the corresponding products could also be achieved (**61 and 62**). Thanks to the slightly lower electrophilic property of the nitryl radical than that of the nitronium ion, the nitrating regioselectivities toward relative electron-rich sites were promoted compared to the "mixed-acid" approach (such as regioselectivities for substrate **57**: *m*:*o* = 4[23] for mixed-acid protocol; only *meta*-isomer obtained for our method).

https://doi.org/10.1021/jacsau.4c00880
JACS Au 2024, 4, 4899−4909

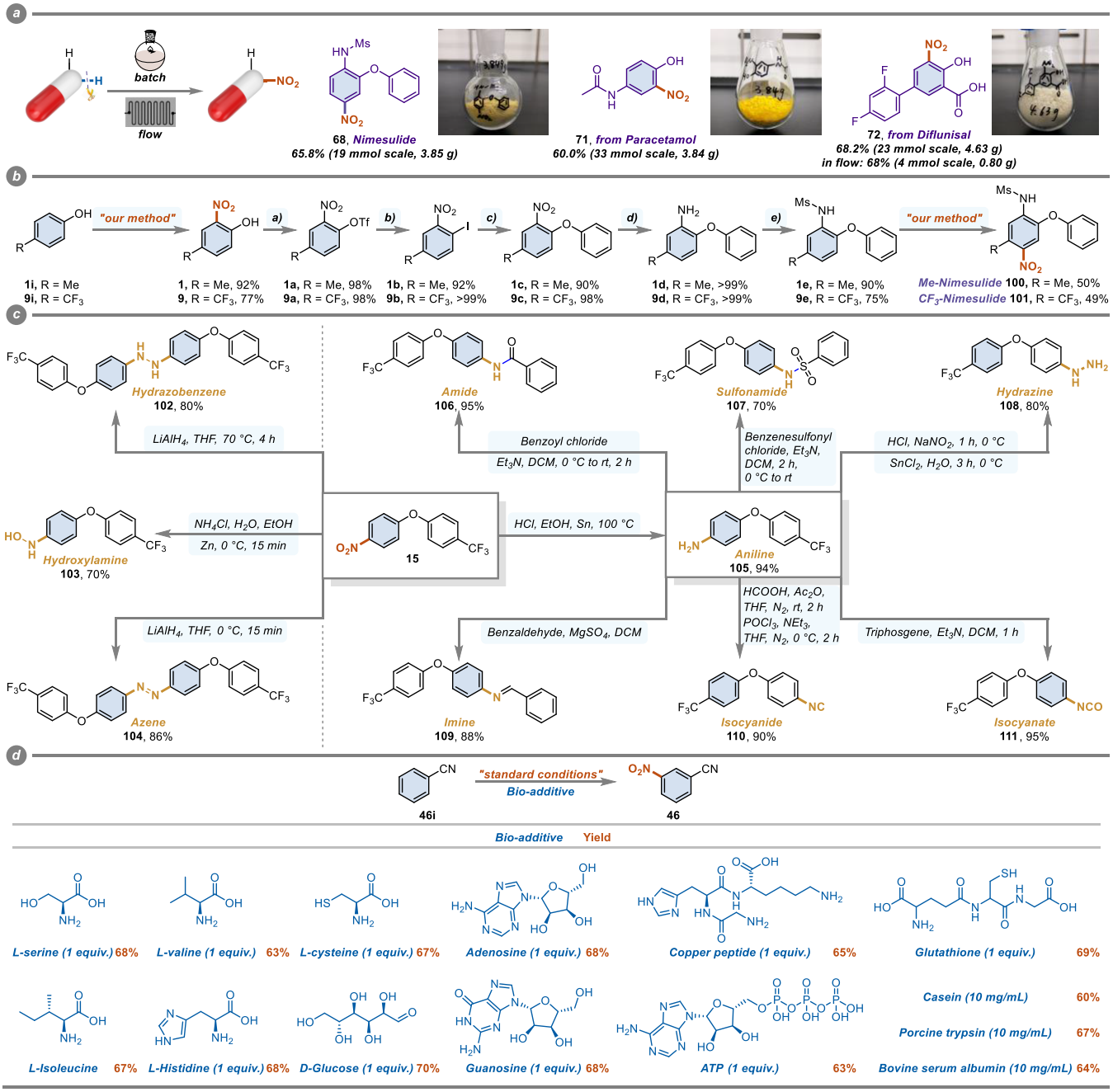

Figure 4. Synthetic applications. (a) Scale-up synthesis of Nimesulide, NO_2−Paracetamol, and NO_2-Diflunisal. (b) Total synthesis of two Nimesulide analogs. (c) Functional-group transformations of the nitrated product. (d) Investigation on the compatibility of bioadditives.

The nitro group is considered to be a unique and key functional group in some drugs such as anticancer, antiparasitic, and antitubercular agents, antibiotics, and tranquilizers.[24] Consequently, expanding the applicable scope to late-stage photonitration of drugs and biorelevant compounds will greatly enhance the application value of our strategy in pharmaceutical and agrochemical discovery and functional molecule modification (Figure 3). For this purpose, a nonsteroidal anti-inflammatory drug, Nimesulide, was successfully synthesized in 66% yield (**68**) first and then was nitrated again under the same conditions in 82% yield (**69**, the structure confirmed with Single-crystal X-ray diffraction[8b]). Sequentially, a vast series of nitrated derivatives of known drugs and bioactive molecules, including Leflunomide (**70**), Paracetamol (**71**), Diflunisal (**72**), *O*-Desmethylvenlafaxine (**73**), Tyrosol (**74**), Gemfibrozil (**75**), Ibuprofen (**76**, **77**), and Naproxen (**78**), were synthesized in good to excellent yields. Nitration conversion of types of biogenic complex molecules was also tried, and the corresponding products from steroids (**79 and 80**), terpenes (**81 and 82**), carbohydrates (**85 and 86**), and fatty acids (**87 and 88**) were all achieved efficiently. Moreover, our protocol was efficaciously applied in nitration of derivates from diversified amino acids including glycine (**89**), L-valine (**90**), L-tyrosine (**91**), L-aspartic acid (**92**), D-lysine (**93**), L-glutamic acid (**94**), D-serine (**95**), and L-proline (**96**), and even those from dipeptides (**97 and 98**) and tripeptides (**99**) were also demonstrated to be suitable substrates, exhibiting foreseeable application of our method in protein

https://doi.org/10.1021/jacsau.4c00880
JACS Au 2024, 4, 4899−4909

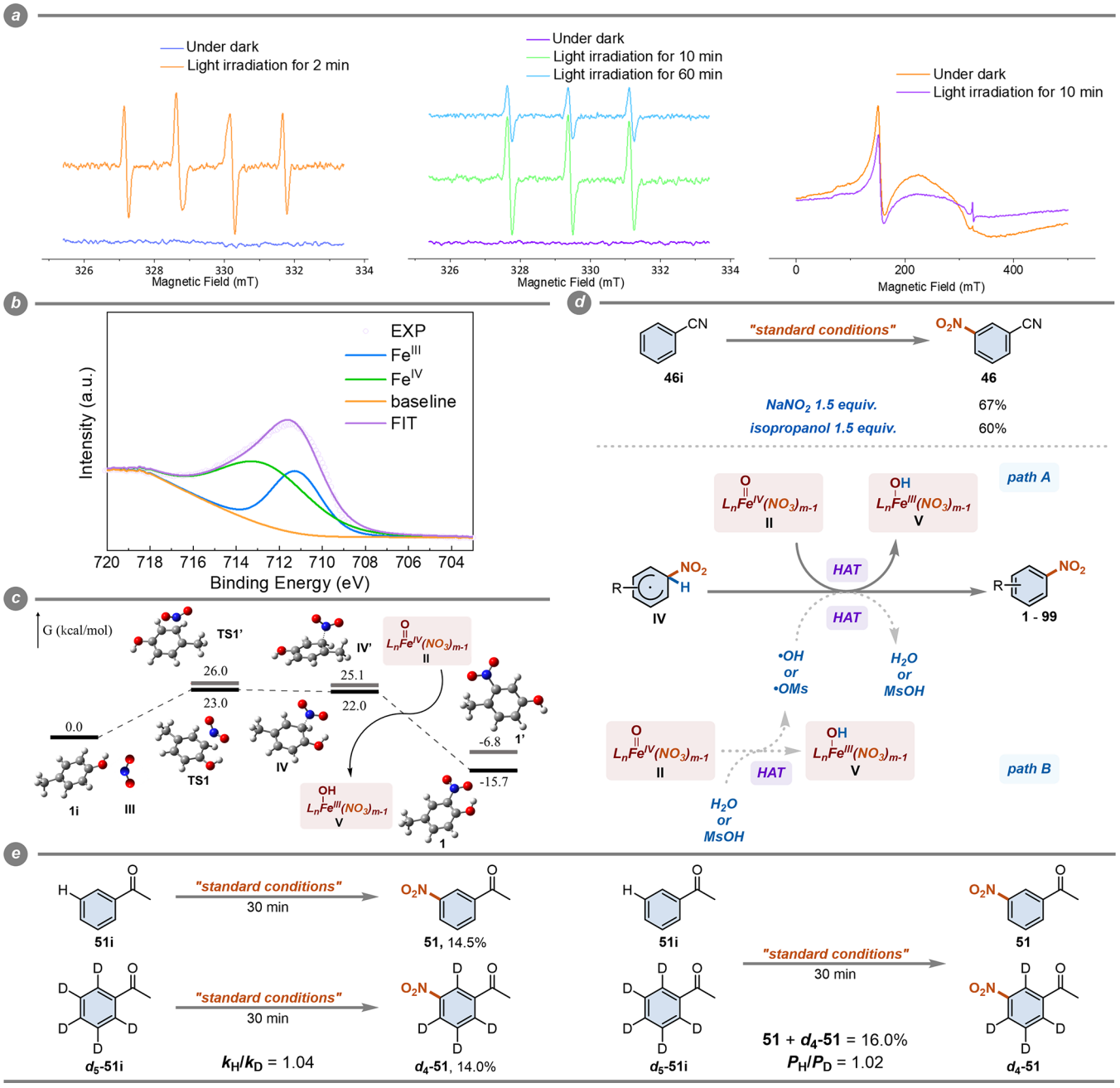

Figure 5. Mechanistic studies. (a) In situ ESR spectra. (b) Fe $2p_{3/2}$ XPS spectra. (c) Computational study of electrophilic aromatic substitution of a nitryl radical. (d) Control experiments with a hydroxyl radical scavenger. (e) KIE studies.

postmodification in situ. Additionally, bisphenol A, a famous polymer monomer of polycarbonates and epoxy resins, was utilized, availably furnishing mono- and dinitrated products under different conditions (**83 and 85**). It is worth mentioning that many complex drug molecules with multiple active functional groups such as Leflunomide (**70**), *O*-Desmethyl-venlafaxine (**73**), etc. are directly nitrated for the first time to our knowledge, and the yields and regioselectivities for many products are improved toward those of the previous state of the art (Table S3), showing the advanced nature of our approach.

Applications and Mechanistic Investigation

Whether a synthetic reaction can be conveniently scaled up is a key factor in evaluating synthetic practicability. For our photonitration system, gram-scale synthesis of **68**, **71**, and **72** was carried out, respectively, in a batch reaction, obtaining 3.85 g of Nimesulide, 3.84 g of NO_2−Paracetamol, and 4.63 g of NO_2-Diflunisal in high purities without obvious loss of efficiency (Figure 4a, details see Figure S11). To further increase the light utilization efficiency, a well-designed continuous-flow photocatalytic microreactor[25] was attempted, capable of affording nitrated Diflunisal **72** in a similar result to that of the batch reaction with a reduced time and attenuated light irradiation (for details, see Figure S12). To further showcase the method's practicability, we applied our strategy to the total synthesis of two never-reported Nimesulide analogs. As a nonsteroidal anti-inflammatory drug with pain medication and fever-reducing properties, Nimesulide is approved for the treatment of acute pain, symptomatic

https://doi.org/10.1021/jacsau.4c00880
JACS Au 2024, 4, 4899−4909

treatment of osteoarthritis, and primary dysmenorrhea.[26] Previous routes to Nimesulide invariably suffered from the use of excess nitric and sulfuric acids under heating. In our protocol shown in Figure 4b, the first nitrogen-introducing step on a substituted phenol ring was performed with our photonitration method (**1 and 9**). After multistep synthesis, our approach was utilized again in the final nitration process, delivering the desired Me-Nimesulide **100** and CF_3−Nimesulide **101** in moderate yields. Our green and sustainable protocol substantially expands the readily accessible chemical space around this scaffold. Furthermore, transformations of the nitro group according to the long-standing studies of its utilization in organic synthesis[1] were presented by using the oxidibenzene derivative **15** (Figure 4c). Upon different reduction conditions, diphenylhydrazine **102**, hydroxylamine **103**, dye-like azo compound **104**, and amine **105** were efficiently generated. Sequentially, acylation and sulfonylation of **105** led to amide **106** and sulfonamide **107**. A two-step oxidation−reduction procedure through a diazonium intermediate transferred **105** to hydrazinobenzene **108** effectively, while a dehydration reaction between **105** and benzaldehyde afforded imine **109** in 88% yield. Isocyanide **110** and isocyanate **111** as active synthons for further couplings were also achieved *via* C1 growth of **105**.

As shown in Figure 3, our photonitration system demonstrated good functional group compatibility, and the next issue that we cared about was its tolerance of different kinds of biochemically important molecules[27] (Figure 4d). When a series of bioadditives including amino acids, monosaccharide, peptide, adenosine triphosphate, and nucleotides were added, they were found to have little influence on the reaction result. In addition to these small molecules, some albumins and enzymes as core macromolecules in organisms were involved as bioadditives in the nitration reaction, and the corresponding nitrated products were supplied in satisfactory yields. These experiments suggest the possible biocompatibility and potential adaptability of the visible-light-driven selective nitration system toward a humoral environment.

To validate our conjecture about the mechanism, several trapping experiments were conducted first. When stoichiometric 2,2,6,6-tetramethylpiperidinooxy (TEMPO), 2,6-di-*tert*-butyl-4-methylphenol (BHT), and 1,1-diphenyl-ethylene were respectively added to the reaction system, the yields of **46** slashed dramatically, which suggested that a radical process was involved (Figure S2). Furthermore, the electron spin-resonance (ESR) experiments were performed to further distinguish the radical category. The ESR spectrum of a mixture of $Fe(NO_3)_3{\cdot}9H_2O$ and diphenyl ether (**14i**) in MeCN with 5, 5-dimethyl-1-pyrroline *N*-oxide (DMPO) as a radical spin trap under dark conditions showed no signal of a trapped radical. After irradiation for 2 min, an obvious quartet-signal (g = 2.0031, a_N = 1.50 mT, a_H = 1.52 mT) was observed, indicating the appearance of a nitryl radical (Figure 5a, left part).[28] To our delight, the $\cdot NO_2$ signal could be directly detected in situ as a triplet-signal (g = 2.0031, a = 1.73 mT) without DMPO after 10 min irradiation, and the intensity of the signal markedly diminished after 60 min illumination which implied the consumption of $\cdot NO_2$ through nitration of **14i** (Figure 5a, middle part). Meanwhile, the variation of the paramagnetic Fe^{III} signal of a saturated solution of $Fe(NO_3)_3{\cdot}9H_2O$ in MeCN at 110 K before and after light irradiation was also explored. The results showed the Fe^{III} signal around 150.7 mT was slightly attenuated by a 10-minute irradiation, suggesting the transformation of a part of Fe^{III} to a diamagnetic species (Figure 5a, right part). Furthermore, X-ray photoelectron spectroscopy (XPS) detection was conducted to figure out the valence state change of iron. As shown in Figure 5b, the peaks located at 711.32 and 712.99 eV in the Fe $2p_{3/2}$ XPS spectra of the iron residue were, respectively, attributed to Fe^{III} and Fe^{IV} according to the reported literature,[29] indicating the system undergoes a Fe^{III}−Fe^{IV} pathway. To further dissect the reaction mechanism, we then studied the detailed procedures of electrophilic aromatic substitution between **1** and a nitryl radical based on density functional theory (DFT) calculations (Figure 5c). The most favorable pathway for radical nitration of **1** consisted of electrophilic addition (**1i-TS1-IV**), followed by spontaneous dehydrogenation through HAT (**IV** to **1**). Notably, the high regioselectivity between ortho- and meta-positions resulted from the distinct Gibbs free energy gaps at the transition state (**TS1**, $\Delta\Delta G^{\ddagger}$ = 3.0 kcal mol^{-1}) and cyclic radical intermediate state (**IV**, $\Delta\Delta G^{\ddagger}$ = 3.1 kcal mol^{-1}). Additionally, hydroxyl radicals that can act as the HAT mediator may also be generated especially in the presence of MsOH. To further investigate this issue, stoichiometric OH radical scavengers ($NaNO_2$ and isopropyl alcohol) were, respectively, added to the MsOH-consisting reaction system. The outcomes showed the yields of **46** slightly decreased, which suggested that the OH radical might make a little contribution inside this system through Path B (Figure 5d).[30] Besides, for electron-deficient arenes, the addition of MsOH may neutralize the resultant hydroxide (**V** to **I** in Figure 1e) and maintain a high concentration of the nitryl radical to overcome the hard electrophilic addition, while the oxygen atmosphere may be helpful for the dehydrogenation process of **IV** through singlet oxygen. Moreover, kinetic isotopic effect (KIE) studies with separate kinetic experiments were employed to gain insights into the C−H cleavage step for this nitration process. The KIE values given by k_H/k_D and P_H/P_D were measured as 1.04 and 1.02 *via* using **51i**/d_5-**51i**, respectively, as substrates (Figure 5e, left part) or a 1:1 mixture of **51i** and d_5-**51i** as substrates (Figure 5e, right part) to produce **51**. These KIE outcomes disclosed that the C−H splitting process did not appear to be a "rate-determining step".[31] A light-on−off experiment was carried out next, revealing that continuous light irradiation was crucial for this transformation (Figure S10).

CONCLUSIONS

The results presented here demonstrate a visible-light-initiated biocompatible arene C−H nitration with high efficiency and regioselectivity, marvelous functional group tolerance and substrate suitability, and wide application in scale-up synthesis, total synthesis, and late-stage modification. A nitryl radical is found to be the key nitrification reagent generated by the unusual β-homolysis of a ferric-nitrate complex. The next phase of these studies will focus on other hypervalent heteroatom-center radicals given by similar β-homolysis of diverse metal-anion complexes, which together could provide the development of a general platform for multitudinous C(sp^2)−H and C(sp^3)−H functionalization of great interest to practitioners of synthetic chemistry in academic and industrial institutes.

https://doi.org/10.1021/jacsau.4c00880
JACS Au 2024, 4, 4899−4909

METHODS

General Procedure for Selective Arene Photonitration

General Procedure I. Arene (0.2 mmol), $Fe(NO_3)_3{\cdot}9H_2O$ (0.08 mmol, 0.4 equiv, 32 mg), and MeCN (2 mL) were added into a 10 mL reaction tube with a magnetic stir bar in sequence. The mixture was allowed to stir under N_2 with irradiation of a 30 W 395 nm LED (1 cm away, with circulating water to keep the reaction at room temperature) for 8 h. Upon completion, the reaction solution was concentrated under reduced pressure, and the residue was purified by silica gel flash column chromatography to give the desired product.

General Procedure II. Arene (0.2 mmol), $Fe(NO_3)_3{\cdot}9H_2O$ (0.3 mmol, 1.5 equiv, 120 mg), MeCN (2 mL) and MsOH (0.22 mmol, 1.1 equiv, 21 mg) were added into a 10 mL reaction tube with a magnetic stir bar in sequence. The mixture was allowed to stir under O_2 with irradiation of a 30 W 395 nm LED (1 cm away, with circulating water to keep the reaction at room temperature) for 8 h. Upon completion, the reaction solution was concentrated under reduced pressure and the residue was purified by silica gel flash column chromatography to give the desired product.

ASSOCIATED CONTENT

Supporting Information

The Supporting Information is available free of charge at https://pubs.acs.org/doi/10.1021/jacsau.4c00880.

Optimizations, synthetic procedures, mechanism investigations, DFT calculations, characterization data, and NMR spectra of synthesized compounds (PDF)

AUTHOR INFORMATION

Corresponding Author

Yunhe Jin − *State Key Laboratory of Fine Chemicals, School of Chemistry, Dalian University of Technology, Dalian 116024, China;* orcid.org/0000-0003-0626-4587; Email: jinyh18@dlut.edu.cn

Authors

Shuyang Liu − *State Key Laboratory of Fine Chemicals, School of Chemistry, Dalian University of Technology, Dalian 116024, China;* orcid.org/0009-0001-8246-4970

Ziyu Gan − *State Key Laboratory of Fine Chemicals, School of Chemistry, Dalian University of Technology, Dalian 116024, China;* orcid.org/0009-0005-0226-0572

Min Jiang − *College of Materials, Chemistry and Chemical Engineering, Hangzhou Normal University, Hangzhou 310036, China*

Qian Liao − *State Key Laboratory of Fine Chemicals, School of Chemistry, Dalian University of Technology, Dalian 116024, China;* orcid.org/0000-0002-0788-9223

Yusheng Lu − *State Key Laboratory of Fine Chemicals, School of Chemistry, Dalian University of Technology, Dalian 116024, China*

Hongyao Wang − *State Key Laboratory of Fine Chemicals, School of Chemistry, Dalian University of Technology, Dalian 116024, China*

Zhiyan Xue − *State Key Laboratory of Fine Chemicals, School of Chemistry, Dalian University of Technology, Dalian 116024, China*

Ziyang Chen − *State Key Laboratory of Fine Chemicals, School of Chemistry, Dalian University of Technology, Dalian 116024, China*

Yongqiang Zhang − *State Key Laboratory of Fine Chemicals, School of Chemistry, Dalian University of Technology, Dalian 116024, China*

Xiaobo Yang − *Institute of Catalysis for Energy and Environment, College of Chemistry and Chemical Engineering, Shenyang Normal University, Shenyang 110034, China;* orcid.org/0000-0003-0684-8419

Chunying Duan − *State Key Laboratory of Coordination Chemistry, Nanjing University, Nanjing 210093, China;* orcid.org/0000-0003-1638-6633

Complete contact information is available at: https://pubs.acs.org/10.1021/jacsau.4c00880

Author Contributions

Y.J. supervised the project and provided guidance on the project. Y.J. and S.L. conceived and designed the study. All authors performed and analyzed the experiments. S.L., M.J., Q.L., and Y.J. wrote and revised the paper. CRediT: **Shuyang Liu** conceptualization, data curation, formal analysis, investigation, methodology, project administration, validation, writing - original draft, writing - review & editing; **Ziyu Gan** investigation, methodology; **Min Jiang** investigation, methodology, writing - original draft, writing - review & editing; **Qian Liao** investigation, methodology, writing - original draft, writing - review & editing; **Yusheng Lu** investigation; **Hongyao Wang** investigation; **Zhiyan Xue** investigation; **Ziyang Chen** investigation; **Yongqiang Zhang** investigation; **Xiaobo Yang** investigation; **Chunying Duan** funding acquisition; **Yunhe Jin** conceptualization, funding acquisition, investigation, methodology, project administration, resources, supervision, writing - original draft, writing - review & editing.

Notes

The authors declare no competing financial interest.

ACKNOWLEDGMENTS

We acknowledge the support of the National Natural Science Foundation of China (grant no. 21901032 to Y.J., grant no. 21890381, 21820102001 to C.D.), the Fundamental Research Funds for the Central Universities (grant no. DUT21LK13 to Y.J.), and the start-up grant from Dalian University of Technology (fellowship to Y.J.). We highly appreciated Pro. Shengyang Tao and Pro. Lijing Zhang in School of Chemistry at Dalian University of Technology for their great help in flow chemistry. We acknowledge the assistance of Dr. Huihui Wan, Dr. Yuming Sun, Dr. Qingxin Yin, and Ms. Chen Wang in DUT Instrumental Analysis Center for their great help in HRMS and Maldi analysis.

REFERENCES

(1) (a) Clayden, J.; Greeves, N.; Warren, S. *Organic chemistry*; Oxford University Press: USA, 2012. (b) Ono, N. *The Nitro Group in Organic Synthesis*; John Wiley & Sons, 2003.

(2) McGrath, N. A.; Brichacek, M.; Njardarson, J. T. A Graphical Journey of Innovative Organic Architectures That Have Improved Our Lives. *J. Chem. Educ.* **2010**, *87*, 1348−1349.

(3) *Nitrobenzene Market: Global Industry Analysis and Forecast (2024−2030)*. www.reportlinker.com/p06032340/Global-Nitrobenzene-Industry (accessed March 2024).

(4) (a) Gutekunst, W. R.; Baran, P. S. C−H functionalization logic in total synthesis. *Chem. Soc. Rev.* **2011**, *40*, 1976−1991. (b) Wencel-Delord, J.; Glorius, F. C−H bond activation enables the rapid construction and late-stage diversification of functional molecules. *Nat. Chem.* **2013**, *5*, 369−375. (c) Cernak, T.; Dykstra, K. D.; Tyagarajan, S.; Vachal, P.; Krska, S. W. The medicinal chemist's toolbox for late stage functionalization of drug-like molecules. *Chem. Soc. Rev.* **2016**, *45*, 546−576. (d) Guillemard, L.; Kaplaneris, N.;

Ackermann, L.; Johansson, M. J. Late-stage C−H functionalization offers new opportunities in drug discovery. *Nat. Rev. Chem.* **2021**, *5*, 522−545.
(5) Hughes, E. D.; Ingold, C. K.; Reed, R. I. Kinetics of Aromatic Nitration: the Nitronium Ion. *Nature* **1946**, *158*, 448−449.
(6) Olah, G. A.; Narang, S. C.; Olah, J. A.; Lammertsma, K. Recent aspects of nitration: New preparative methods and mechanistic studies (A Review). *Proc. Natl. Acad. Sci. U. S. A.* **1982**, *79*, 4487−4494.
(7) (a) Yan, G.; Yang, M. Recent advances in the synthesis of aromatic nitro compounds. *Org. Biomol. Chem.* **2013**, *11*, 2554−2566. (b) Song, L.-R.; Fan, Z.; Zhang, A. Recent advances in transition metal-catalyzed C(sp^2)−H nitration. *Org. Biomol. Chem.* **2019**, *17*, 1351−1361. (c) Patel, S. S.; Patel, D. B.; Patel, H. D. Synthetic Protocols for Aromatic Nitration: A Review. *ChemistrySelect* **2021**, *6*, 1337−1356. (d) Patra, S.; Mosiagin, I.; Giri, R.; Katayev, D. Organic Nitrating Reagents. *Synthesis* **2022**, *54*, 3432−3472.
(8) (a) Calvo, R.; Zhang, K.; Passera, A.; Katayev, D. Facile access to nitroarenes and nitroheteroarenes using N-nitrosaccharin. *Nat. Commun.* **2019**, *10*, 3410. (b) Yang, T.; Li, X.; Deng, S.; Qi, X.; Cong, H.; Cheng, H.-G.; Shi, L.; Zhou, Q.; Zhuang, L. From N−H Nitration to Controllable Aromatic Mononitration and Dinitration−The Discovery of a Versatile and Powerful N-Nitropyrazole Nitrating Reagent. *JACS Au* **2022**, *2*, 2152−2161. (c) Jia, F.; Li, A.; Hu, X. Dinitro-5,5-Dimethylhydantoin: An Arene Nitration Reagent. *Org. Lett.* **2023**, *25*, 4605−4609. (d) Zheng, Y.; Hu, Q.-Q.; Huang, Q.; Xie, Y. Late-Stage C−H Nitration of Unactivated Arenes by $Fe(NO_3)_3$·$9H_2O$ in Hexafluoroisopropanol. *Org. Lett.* **2024**, *26*, 3316−3320. (e) Wu, Y.; Lu, W.; Ma, Y.-N.; Chen, F.; Ren, W.; Chen, X. Trifluoromethanesulfonic Acid Promoted Controllable Electrophilic Aromatic Nitration. *J. Org. Chem.* **2023**, *88*, 11322−11327. (f) Wu, C.; Bian, Q.; Ding, T.; Tang, M.; Zhang, W.; Xu, Y.; Liu, B.; Xu, H.; Li, H.-B.; Fu, H. Photoinduced Iron-Catalyzed *ipso*-Nitration of Aryl Halides via Single-Electron Transfer. *ACS Catal.* **2021**, *11*, 9561−9568. (g) He, Y.; Zhao, N.; Qiu, L.; Zhang, X.; Fan, X. Regio- and Chemoselective Mono- and Bisnitration of 8-Amino quinoline Amides with $Fe(NO_3)_3$·$9H_2O$ as Promoter and Nitro Source. *Org. Lett.* **2016**, *18*, 6054−6057. (h) Chen, X.-H.; Ma, D.-D.; Gao, X.; Li, Y.-M.; Jiang, D.-B.; Ma, C.; Cui, H.-L. Nitration of Pyrrolo[2,1-*a*]isoquinolines. *J. Org. Chem.* **2023**, *88*, 4649−4661. (i) Yang, X.; Wang, B.; Zhang, Q.; Szekely, A.; Wu, M.; Li, Y. Nitration of Derivatives of Imidazo[1,5-a]pyridine *via* C−H Functionalization with $Fe(NO_3)_3$·$9H_2O$ as a Promoter and a Nitro Source. *ChemistrySelect* **2024**, *9*, No. e202401114.
(9) (a) Liu, Y.-K.; Lou, S.-J.; Xu, D.-Q.; Xu, Z.-Y. Regiospecific Synthesis of Nitroarenes by Palladium-Catalyzed Nitrogen-Donor-Directed Aromatic C−H Nitration. *Chem.−Eur. J.* **2010**, *16*, 13590−13593. (b) Liang, Y.-F.; Li, X.; Wang, X.; Yan, Y.; Feng, P.; Jiao, N. Aerobic Oxidation of Pd^{II} to Pd^{IV} by Active Radical Reactants: Direct C−H Nitration and Acylation of Arenes *via* Oxygenation Process with Molecular Oxygen. *ACS Catal.* **2015**, *5*, 1956−1963. (c) Saxena, P.; Kapur, M. Cobalt-Catalyzed C−H Nitration of Indoles by Employing a Removable Directing Group. *Chem.−Asian J.* **2018**, *13*, 861−870.
(10) (a) Wan, L.; Qiao, K.; Yuan, X.; Zheng, M.-W.; Fan, B.-B.; Di, Z. C.; Zhang, D.; Fang, Z.; Guo, K. Nickel-Catalyzed Regioselective C−H Bond Mono- and Bis-Nitration of Aryloxazolines with *tert*-Butyl Nitrite as Nitro Source. *Adv. Synth. Catal.* **2017**, *359*, 2596−2604. (b) Chaudhary, P.; Gupta, S.; Muniyappan, N.; Sabiah, S.; Kandasamy, J. Regioselective Nitration of *N*-Alkyl Anilines using *tert*-Butyl Nitrite under Mild Condition. *J. Org. Chem.* **2019**, *84*, 104−119. (c) Kianmehr, E.; Nasab, S. B. Silver-Catalyzed Chemo- and Regioselective Nitration of Anilides. *Eur. J. Org. Chem.* **2018**, *2018*, 6447−6452. (d) Blum, S. P.; Nickel, C.; Schäffer, L.; Karakaya, T.; Waldvogel, S. R. Electrochemical Nitration with Nitrite. *ChemSusChem* **2021**, *14*, 4936−4940. (e) Long, T.; Liu, L.; Tao, Y.; Zhang, W.; Quan, J.; Zheng, J.; Hegemann, J. D.; Uesugi, M.; Yao, W.; Tian, H.; Wang, H. Light-Controlled Tyrosine Nitration of Proteins. *Angew. Chem., Int. Ed.* **2021**, *60*, 13414−13422. (f) Patra, S.; Mosiagin, I.; Giri, R.; Nauser, T.; Katayev, D. Electron-Driven Nitration of Unsaturated Hydrocarbons. *Angew. Chem., Int. Ed.* **2023**, *62*, No. e202300533.
(11) (a) Stephenson, C. R.; Yoon, T. P.; MacMillan, D. W. *Visible light photocatalysis in organic chemistry*; John Wiley & Sons: 2018. (b) Skubi, K. L.; Blum, T. R.; Yoon, T. P. Dual Catalysis Strategies in Photochemical Synthesis. *Chem. Rev.* **2016**, *116*, 10035−10074. (c) Romero, N. A.; Nicewicz, D. A. Organic Photoredox Catalysis. *Chem. Rev.* **2016**, *116*, 10075−10166. (d) Xuan, J.; Xiao, W.-J. Visible-Light Photoredox Catalysis. *Angew. Chem., Int. Ed.* **2012**, *51*, 6828−6838.
(12) (a) Wenger, O. S. Photoactive Complexes with Earth-Abundant Metals. *J. Am. Chem. Soc.* **2018**, *140*, 13522−13533. (b) Abderrazak, Y.; Bhattacharyya, A.; Reiser, O. Visible-Light-Induced Homolysis of Earth-Abundant Metal-Substrate Complexes: A Complementary Activation Strategy in Photoredox Catalysis. *Angew. Chem., Int. Ed.* **2021**, *60*, 21100−21115.
(13) Shields, B. J.; Doyle, A. G. Direct C(sp^3)−H Cross Coupling Enabled by Catalytic Generation of Chlorine Radicals. *J. Am. Chem. Soc.* **2016**, *138*, 12719−12722.
(14) Heitz, D. R.; Tellis, J. C.; Molander, G. A. Photochemical Nickel-Catalyzed C−H Arylation: Synthetic Scope and Mechanistic Investigations. *J. Am. Chem. Soc.* **2016**, *138*, 12715−12718.
(15) Campbell, B. M.; Gordon, J. B.; Raguram, E. R.; Gonzalez, M. I.; Reynolds, K. G.; Nava, M.; Nocera, D. G. Electrophotocatalytic perfluoroalkylation by LMCT excitation of Ag (II) perfluoroalkyl carboxylates. *Science* **2024**, *383*, 279−284.
(16) (a) Hu, A.; Guo, J.-J.; Pan, H.; Zuo, Z. Selective functionalization of methane, ethane, and higher alkanes by cerium photocatalysis. *Science* **2018**, *361*, 668−672. (b) Wen, L.; Ding, J.; Duan, L.; Wang, S.; An, Q.; Wang, H.; Zuo, Z. Multiplicative enhancement of stereoenrichment by a single catalyst for deracemization of alcohols. *Science* **2023**, *382*, 458−464.
(17) (a) Treacy, S. M.; Rovis, T. Copper catalyzed C(sp^3)−H bond alkylation via photoinduced ligand-to-metal charge transfer. *J. Am. Chem. Soc.* **2021**, *143*, 2729−2735. (b) Sang, R.; Han, W.; Zhang, H.; Saunders, C. M.; Noble, A.; Aggarwal, V. K. Copper-mediated dehydrogenative C(sp^3)−H borylation of alkanes. *J. Am. Chem. Soc.* **2023**, *145*, 15207−15217. (c) Wang, M.; Huang, Y.; Hu, P. Terminal C(sp^3)−H borylation through intermolecular radical sampling. *Science* **2024**, *383*, 537−544. (d) Jin, Y.; Zhang, Q.; Wang, L.; Wang, X.; Meng, C.; Duan, C. Convenient C(sp^3)−H bond functionalisation of light alkanes and other compounds by iron photocatalysis. *Green Chem.* **2021**, *23*, 6984−6989. (e) Jin, Y.; Wang, L.; Zhang, Q.; Zhang, Y.; Liao, Q.; Duan, C. Photo-induced direct alkynylation of methane and other light alkanes by iron catalysis. *Green Chem.* **2021**, *23*, 9406−9411. (f) Zhang, Q.; Liu, S.; Lei, J.; Zhang, Y.; Meng, C.; Duan, C.; Jin, Y. Iron-Catalyzed Photoredox Functionalization of Methane and Heavier Gaseous Alkanes: Scope, Kinetics, and Computational Studies. *Org. Lett.* **2022**, *24*, 1901−1906. (g) Chen, T. Q.; Pedersen, P. S.; Dow, N. W.; Fayad, R.; Hauke, C. E.; Rosko, M. C.; Danilov, E. O.; Blakemore, D. C.; Dechert-Schmitt, A.-M.; Knauber, T. A unified approach to decarboxylative halogenation of (Hetero) aryl carboxylic acids. *J. Am. Chem. Soc.* **2022**, *144*, 8296−8305. (h) Dow, N. W.; Pedersen, P. S.; Chen, T. Q.; Blakemore, D. C.; Dechert-Schmitt, A.-M.; Knauber, T.; MacMillan, D. W. Decarboxylative borylation and cross-coupling of (hetero) aryl acids enabled by copper charge transfer catalysis. *J. Am. Chem. Soc.* **2022**, *144*, 6163−6172. (i) Xu, P.; López-Rojas, P.; Ritter, T. Radical decarboxylative carbometalation of benzoic acids: a solution to aromatic decarboxylative fluorination. *J. Am. Chem. Soc.* **2021**, *143*, 5349−5354. (j) Su, W.; Xu, P.; Ritter, T. Decarboxylative hydroxylation of benzoic acids. *Angew. Chem., Int. Ed.* **2021**, *60*, 24012−24017. (k) Chinchole, A.; Henriquez, M. A.; Cortes-Arriagada, D.; Cabrera, A. R.; Reiser, O. Iron (III)-light-induced homolysis: A dual photocatalytic approach for the hydroacylation of alkenes using acyl radicals via direct HAT from aldehydes. *ACS Catal.* **2022**, *12*, 13549−13554. (l) Birnthaler, D.; Narobe, R.; Lopez-Berguno, E.; Haag, C.; König, B. Synthetic Application of Bismuth LMCT Photocatalysis in Radical Coupling Reactions. *ACS Catal.*

https://doi.org/10.1021/jacsau.4c00880
JACS Au 2024, 4, 4899−4909

2023, *13*, 1125−1132. (m) Fernández-García, S.; Chantzakou, V. O.; Juliá-Hernández, F. Direct Decarboxylation of Trifluoroacetates Enabled by Iron Photocatalysis. *Angew. Chem., Int. Ed.* **2024**, *63*, No. e202311984. (n) Lutovsky, G. A.; Gockel, S. N.; Bundesmann, M. W.; Bagley, S. W.; Yoon, T. P. Iron-mediated modular decarboxylative cross-nucleophile coupling. *Chem.* **2023**, *9*, 1610−1621. (o) Li, Q. Y.; Gockel, S. N.; Lutovsky, G. A.; DeGlopper, K. S.; Baldwin, N. J.; Bundesmann, M. W.; Tucker, J. W.; Bagley, S. W.; Yoon, T. P. Decarboxylative cross-nucleophile coupling via ligand-to-metal charge transfer photoexcitation of Cu (II) carboxylates. *Nat. Chem.* **2022**, *14*, 94−99. (p) Bian, K.-J.; Lu, Y.-C.; Nemoto, D., Jr; Kao, S.-C.; Chen, X.; West, J. G. Photocatalytic hydrofluoroalkylation of alkenes with carboxylic acids. *Nat. Chem.* **2023**, *15*, 1683−1692. (q) Bian, K.-J.; Kao, S.-C.; Nemoto, D., Jr; Chen, X.-W.; West, J. G. Photochemical diazidation of alkenes enabled by ligand-to-metal charge transfer and radical ligand transfer. *Nat. Commun.* **2022**, *13*, 7881. (r) Zhang, M.; Zhang, J.; Li, Q.; Shi, Y. Iron-mediated ligand-to-metal charge transfer enables 1, 2-diazidation of alkenes. *Nat. Commun.* **2022**, *13*, 7880. (s) Lindner, H.; Amberg, W. M.; Carreira, E. M. Iron-Mediated Photochemical Anti-Markovnikov Hydroazidation of Unactivated Olefins. *J. Am. Chem. Soc.* **2023**, *145*, 22347−22353. (t) Guo, J.-J.; Hu, A.; Chen, Y.; Sun, J.; Tang, H.; Zuo, Z. Photocatalytic C−C Bond Cleavage and Amination of Cycloalkanols by Cerium(III) Chloride Complex. *Angew. Chem., Int. Ed.* **2016**, *55*, 15319−15322. (u) Hu, A.; Guo, J.-J.; Pan, H.; Tang, H.; Gao, Z.; Zuo, Z. δ-Selective Functionalization of Alkanols Enabled by Visible-Light-Induced Ligand-to-Metal Charge Transfer. *J. Am. Chem. Soc.* **2018**, *140*, 1612−1616. (v) de Groot, L. H. M.; Ilic, A.; Schwarz, J.; Wärnmark, K. Iron Photoredox Catalysis−Past, Present, and Future. *J. Am. Chem. Soc.* **2023**, *145*, 9369−9388. (w) Messinis, A. M.; von Münchow, T.; Surke, M.; Ackermann, L. Room temperature photo-promoted iron-catalysed arene C−H alkenylation without Grignard reagents. *Nat. Catal.* **2024**, *7*, 273−284. (x) Klöpfer, V.; Chinchole, A.; Reiser, O. Dual iron- and organophotocatalyzed hydroformylation, hydroacylation and hydrocarboxylation of Michael-acceptors utilizing 1,3,5-trioxanes as C1-Synthone. *Tetrahedron Chem.* **2024**, *10*, No. 100073. (y) Reichle, A.; Reiser, O. Light-induced homolysis of copper(ii)-complexes−a perspective for photocatalysis. *Chem. Sci.* **2023**, *14*, 4449−4462.

(18) (a) Carlsen, C. U.; Møller, J. K. S.; Skibsted, L. H. Heme-iron in lipid oxidation. *Coord. Chem. Rev.* **2005**, *249*, 485−498. (b) Ortiz de Montellano, P. R. Hydrocarbon Hydroxylation by Cytochrome P450 Enzymes. *Chem. Rev.* **2010**, *110*, 932−948. (c) Shaik, S.; Lai, W.; Chen, H.; Wang, Y. The Valence Bond Way: Reactivity Patterns of Cytochrome P450 Enzymes and Synthetic Analogs. *Acc. Chem. Res.* **2010**, *43*, 1154−1165.

(19) Pedley, J. B. *Thermochemical data of organic compounds*; Springer Science and Business Media, 2012.

(20) (a) Chen, M. S.; White, M. C. A predictably selective aliphatic C−H oxidation reaction for complex molecule synthesis. *Science* **2007**, *318*, 783−787. (b) Chen, M. S.; White, M. C. Combined effects on selectivity in Fe-catalyzed methylene oxidation. *Science* **2010**, *327*, 566−571.

(21) Cheng, L.; Wang, H.; Cai, H.; Zhang, J.; Gong, X.; Han, W. Iron-catalyzed arene C−H hydroxylation. *Science* **2021**, *374*, 77−81.

(22) Patra, S.; Giri, R.; Katayev, D. Nitrative Difunctionalization of Alkenes via Cobalt-Mediated Radical Ligand Transfer and Radical-Polar Crossover Photoredox Catalysis. *ACS Catal.* **2023**, *13*, 16136−16147.

(23) Parnes, H.; Huang, G. T.; Shelton, E. J. Synthesis of [^{14}C]-labelled dihydropyridine calcium channel entry blockers: Nicardipine-[4-^{14}C] and RS-93522-[4-^{14}C]. *J. Labelled Compd. Radiopharm.* **1988**, *25*, 621−626.

(24) Nepali, K.; Lee, H.-Y.; Liou, J.-P. Nitro-Group-Containing Drugs. *J. Med. Chem.* **2019**, *62*, 2851−2893.

(25) Buglioni, L.; Raymenants, F.; Slattery, A.; Zondag, S. D. A.; Noël, T. Technological Innovations in Photochemistry for Organic Synthesis: Flow Chemistry, High-Throughput Experimentation, Scale-up, and Photoelectrochemistry. *Chem. Rev.* **2022**, *122*, 2752−2906.

(26) *Drug Record Nimesulide*. web.archive.org/web/20171223043951/https://livertox.nih.gov/Nimesulide.htm.

(27) Anhäuser, L.; Teders, M.; Rentmeister, A.; Glorius, F. Bio-additive-based screening: toward evaluation of the biocompatibility of chemical reactions. *Nat. Protoc.* **2019**, *14*, 2599−2626.

(28) Buettner, G. R. Spin Trapping: ESR parameters of spin adducts 1474 1528V. *Free Radical Biol. Med.* **1987**, *3*, 259−303.

(29) Li, M.; Li, H.; Ling, C.; Shang, H.; Wang, H.; Zhao, S.; Liang, C.; Mao, C.; Guo, F.; Zhou, B.; Ai, Z.; Zhang, L. Highly selective synthesis of surface Fe^{IV}=O with nanoscale zero-valent iron and chlorite for efficient oxygen transfer reactions. *Proc. Natl. Acad. Sci. U. S. A.* **2023**, *120*, No. e2304562120.

(30) Mack, J.; Bolton, J. R. Photochemistry of nitrite and nitrate in aqueous solution: a review. *J. Photochem. Photobiol., A* **1999**, *128*, 1−13.

(31) Simmons, E. M.; Hartwig, J. F. On the Interpretation of Deuterium Kinetic Isotope Effects in C−H Bond Functionalizations by Transition-Metal Complexes. *Angew. Chem., Int. Ed.* **2012**, *51*, 3066−3072.

https://doi.org/10.1021/jacsau.4c00880
JACS Au 2024, 4, 4899−4909